Journal of Hydroscience and Hydraulic Engineering
Vol. 22, No.2 November, 2004, 155-169

LONG-TERM RUNOFF CALCULATION CONSIDERING CHANGE OF SNOW PACK CONDITION

By

M. Nakatsugawa

Director, Water Environmental Engineering Division,

Civil Engineering Research Institute of Hokkaido, Sapporo, Japan

and

K. Hoshi

Senior Managing Director,

Foundation of Hokkaido River Disaster Prevention Research Center, Sapporo, Japan

SYNOPSIS

In order to conduct adaptive water management for an entire watershed, long-term hydrologic conditions must be examined thoroughly. Hydrologic processes related to snow play a particularly important role in cold, snowy regions. Therefore, reliable estimates of snow accumulation and snowmelt are needed to perform effective water management, while evapotranspiration is also necessary to determine the water budget in an entire watershed. This paper focuses on the hydrologic processes reproduced by a Two-layer Model that deals with the heat balance in the atmosphere, in the vegetation layer and at the ground surface, as well as long-term runoff characteristics calculated by the Tank Model. The proposed method successfully quantified the change of snow cover in relation to the evaluation of hydrologic cycle as well as the effects of vegetation on the hydrological processes using routine meteorological data. Moreover, the Two-layer Model integrated the effects of changes in snow cover and the Tank Model was properly fine-tuned, so that the long-term hydrological factors and hydrologic cycle of a cold, snowy region were accurately simulated.

INTRODUCTION

For water management that contributes to a sound hydrologic cycle, long-term hydrological factors must be understood. Runoff patterns during floods are greatly affected by water storage conditions of the basin, and the assessment of runoff necessitates the development of a long-term runoff model to clarify the water balance of the basin.

Quantification of snow-related hydrological factors is essential, especially in any long-term runoff model for cold, snowy regions. Many runoff models that have been constructed thus far incorporate the effects of snowmelt water. The models proposed by Kondo *et al.* (8) and Yamazaki *et al.* (14) address snow cover and snowmelt water. Bathurst *et al.* (2) made comprehensive research on the water balance of the basin, including snowmelt water. However, an accurate estimation of snow cover and snowmelt water for their integration into analysis of the water balance of the basin is difficult for several reasons:

1) It is difficult to estimate snowfall for the entire basin.
2) Assessment of snow density (water equivalent of snow pack divided by snow depth) is difficult.
3) Infiltration of snowmelt water, in other words, the storage effect of snow cover, is affected by the conditions of snow cover. Accordingly, it changes with time.
4) Without knowing whether snow cover is present, the ground surface conditions (albedo, soil temperature, etc.) cannot be appropriately assessed, and accurate estimation of evapotranspiration, an essential element of water balance in a basin, is not possible.

In short, the conditions of snow cover, including its presence or absence, must be properly assessed, because they influence heat transport between the atmosphere and the ground surface and because water is

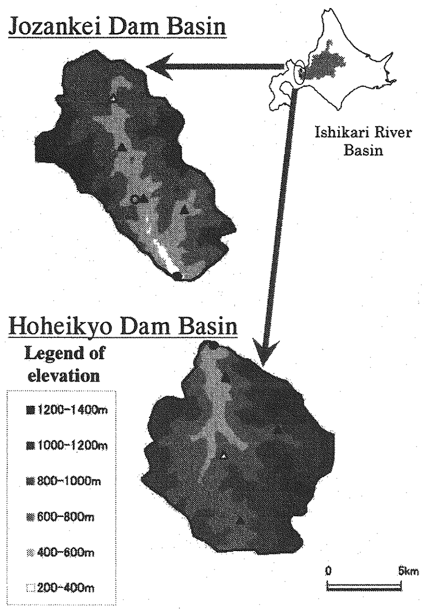

Jozankei Dam Basin (Basin Area; 104km^2)

	Name of observation site (Number of site)		Observation Items
●	Dam Management Office	(1)	Precipitation
			Snow Depth
			Wind Velocity
			Humidity
			Atmospheric Temperature
			Solar Radiation
			Sunshine Duration
			Inflow to Dam Reservoir
▲	Telemetry Site	(3)	Precipitation
△	Telemetry Site with Snow Gauge	(1)	Precipitation
			Snow Depth
○	Driftwood Treatment Plant	(1)	Precipitation
			Snow Depth
			Snow Temperature
			Snowmelt From Snow Cover
			Wind Velocity
			Humidity
			Atmospheric Temperature
			Solar Radiation

Hoheikyo Dam Basin (Basin Area; 134km^2)

	Name of observation site (Number of site)		Observation Items
●	Dam Management Office	(1)	Precipitation
			Snow Depth
			Wind Velocity
			Humidity
			Atmospheric Temperature
			Inflow to Dam Reservoir
▲	Telemetry Site	(3)	Precipitation
△	Telemetry Site with Snow Gauge	(1)	Precipitation
			Snow Depth

Fig. 1 Location of observation site and data item

stored in snow cover during snowmelt runoff. If conditions are not properly assessed, the reproduced water balance and runoff of the entire basin are unlikely to be accurate. Therefore, hydrological factors relevant to water balance were estimated. To make this estimation, the following procedures were carried out:

1) The observed rainfall and snowfall were corrected with respect to elevation and weighted area of observation site so as to make their values accurate throughout the basin.
2) The two-layer model proposed by Kondo *et al.* (8) was adopted to calculate heat flux between atmosphere and ground surface including vegetation, from which snowmelt amount and evapotranspiration were computed.
3) The water equivalent of snow pack was calculated from the balance of snowfall and snowmelt amount (plus evapotranspiration), and the depth and density of snow pack were calculated.

As a result of the above, hydrological factors of dam basins (precipitation, evapotranspiration, snowmelt etc.) were calculated for several years. The validity of these items was evaluated comprehensively. For this evaluation, we examined whether the difference between precipitation and inflow into the dam should be defined as evapotranspiration. Furthermore, we examined how closely the reproduced values of depth of snow pack and water equivalent of snow pack agreed with their measured values.

Runoff was then calculated from the aforementioned calculated values of rainfall, snowmelt amount, and evapotranspiration. The Tank Model was employed to reproduce a long-term runoff. Recently, genetic algorithms (Tanakamaru (12)) and other methods have been proposed for determining the parameters of the Tank model. In our research, we used the Newton-Raphson method, which allows convergence of parameters. Before employing this method, parameters related to groundwater runoff were determined using the filter-separation auto-regressive (AR) method (Hino *et al.* (5)). The purpose was to streamline the parameter determination process of the Newton-Raphson method.

In view of the above, factors related to snow cover were assessed, since those factors affects snowmelt water storage, and runoff was calculated in relation to the water balance of the basin. Our research model uses routine meteorological data measured by dam management offices, thus it is of practical use.

STUDY AREAS AND OBSERVATION DATA

Our research was conducted on two basins in Hokkaido, Japan (Fig. 1): the Jozankei Dam basin (104 km^2) and Hoheikyo Dam basin (134 km^2). Two dams are multi-purpose dams managed by the Hokkaido Development Bureau of the Ministry of Land, Infrastructure and Transport, for flood control, hydroelectric power generation, and water supply. These basins are situated at the upper reaches of the Toyohira River, and the dams supply most of the drinking water of Sapporo City (pop. 1.8 million) as well as providing flood control to urban areas downstream on the Toyohira River. Hence, it is important to estimate precisely the amount of inflow to the dam. In cold, snowy regions such as Hokkaido, the hydrologic processes related to snow play an important role. In the case of the Toyohira River, we have outflow of 1,600 mm per year and precipitation of 2,100 mm. Effective water management requires the estimation of amounts of evapotranspiration and snowmelt according to land use or climate conditions.

Fig. 1 shows the location of observation sites and data items. Our research is based on daily analysis, and the following calculations basically employ routine data from dam management offices and telemetry systems (the black circles, black triangles and white triangles in the figure.), including those on precipitation, wind speed, solar radiation, sunshine duration, humidity, temperature, and snow depth. From the viewpoint of land use, we note that the forests of these basins are characteristic of cold, snowy regions since they have many coniferous trees and few deciduous trees.

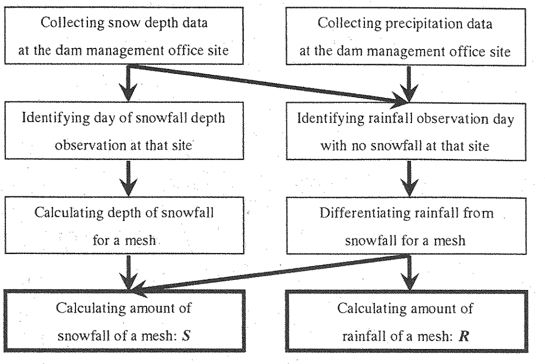

Fig.2 Estimation method of precipitation in the basin

ESTIMATION OF HYDROLOGICAL PROCESSES WITH CHANGE OF SNOW COVER

Estimation of Precipitation

To clarify the water balance of the basin, hydrological factors (precipitation and snowfall) are estimated according to the procedure in Fig. 2. In this report, precipitation is estimated on the basis of elevation. Based on data from the dam management office, rainfall and snowfall (depth of new snowfall) in each grid with 1km by 1km were estimated. These estimates were made by means of regression equations (Kuchizawa *et al.* (9)) (Equation 1):

$$\begin{aligned}&\text{Rainfall}; R_i = a_1 X_{1i} + a_2 X_2 = a_1 X_1 + a_2[\lambda R_0]\\&\text{Snowfall}; S_i = S_1[b_1 \ln(H_{ri}) + b_2]\end{aligned} \qquad (1)$$

where R_i is daily precipitation of mesh i (mm/d), X_{1i} is elevation of mesh i (m), X_2 indicating basin mean precipitation (mm/d) is provided by multiplying the daily precipitation at the dam management office site (R_0) by a weighting factor (λ) , a_1 and a_2 are multiple regression coefficients, S_i is snowfall depth of mesh i (cm/d), S_1 is daily snowfall depth estimated by the difference of snow depth from that day and the previous day at the dam management office site (cm/d), H_{ri} is ratio of elevation of mesh i to elevation of the dam management office site, and b_1 and b_2 are regression coefficients. Then, λ is given by Equation 2:

$$\lambda = \sum_{i=1}^{n} \alpha_i \beta_i \qquad (2)$$

where α_i is the Thiessen coefficient of telemetry observation site i in the basin, and β_i is regression coefficient computed from the relationship between the rainfall at the dam management office site and that at observation site i.

The average rainfall of the basin calculated by Equation 1 is roughly equal to that calculated by the Thiessen method. For observation of rainfall at a dam site, precipitation should be categorized as rainfall or snowfall for each mesh. The reference temperature, T_c (°C) for categorization as rainfall or snowfall, proposed by Kondo *et al.* (8) in following equation, was adopted accordingly.

$$T_c \cong 7.7 - 6.6rh, \qquad \text{at } 0.4 < rh \le 1.0 \qquad (3)$$

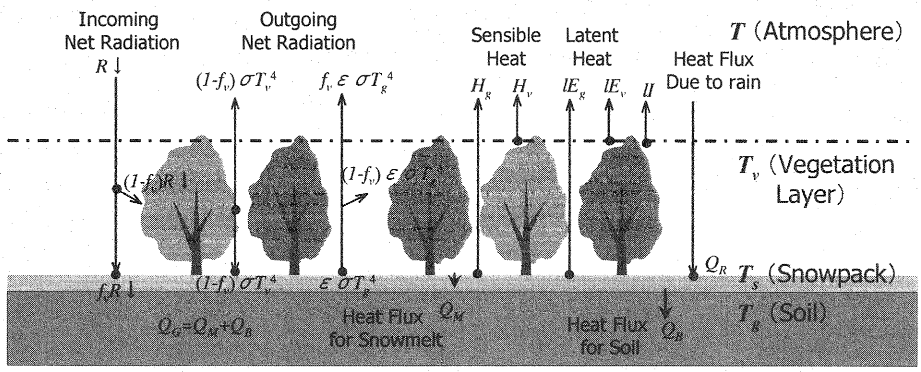

Fig. 3. Schematic figure of the two-layer model

where rh is relative humidity. When the temperature exceeds the reference temperature, T_c, precipitation is categorized as rainfall. When it is lower than that reference, precipitation is categorized as snowfall. Then, the temperature for each mesh is obtained by correcting the observed temperature at the dam management office with the elevation using the lapse rate, 0.65°C/100m. The density of newly fallen snow, used for conversion of depth of snowfall into water equivalent of snowfall, ranges from about 50 to 200 kg/m^3 (Bras (3)). Based on this information and water budget until the end of snowmelt season, snowfall density was here set as 160 kg/m^3. As in the case of rainfall, the water equivalent of snowfall was estimated for each mesh.

Estimation of Evapotranspiration

Evapotranspiration changes dynamically depending on conditions of groundcover and vegetation. For accurate estimation of heat flux, the two-layer model (Fig. 3) proposed by Kondo *et al.* (8) was employed. Equation 4 was formulated to estimate the heat balance at ground surface, and Equation 5 to estimate that at vegetation layer. Interception evaporation is included in these equations:

$$f_V R\downarrow +(1-f_V)\sigma T_V^{\,4} - Q_G + Q_R = \varepsilon\sigma T_g^{\,4} + H_g + \ell E_g \tag{4}$$

$$(1-f_V)(R\downarrow +\varepsilon\sigma T_g^{\,4}) = 2(1-f_V)\sigma T_v^{\,4} + H_v + \ell(E_v + I) \tag{5}$$

where f_v is transmissivity of the vegetation based on radiation, $R\downarrow$ is downward net radiation (W/m^2), Q_G is heat flux provided to the ground surface(W/m^2), Q_R is heat flux provided by rainfall (W/m^2), H_g is sensible heat flux from ground surface (including snow surface) (W/m^2), H_v is sensible heat flux from vegetation layer (W/m^2), lE_g is latent heat flux from ground surface (including snow surface) (W/m^2), lE_v is latent heat flux from vegetation layer (W/m^2), I is evaporation due to interception formulated by Kondo *et al.* (8), T_g is mean temperature of ground surface (including snow surface) (K), T_v is mean temperature of vegetation layer(K), ε is emissivity (1.00 on the ground and 0.97 on snow cover surface), and σ is Stefan-Boltzmann coefficient (5.67 x 10^{-8} W/m^2/K^4).

Then, parameter f_v is expressed by the following equation:

$$f_v = \exp(-F\cdot LAI) \tag{6}$$

where F is a coefficient expressing the relationship between leaf surface slope and incident angle of radiation. To assume a state of isotropy, 0.5 was assigned to F. LAI stands for Leaf Area Index, to which mesh value of each month estimated by Ishii *et al.* (6) is assigned.

A downward net radiation flux is provided by following equation:

$$R\downarrow = (1-\alpha)S\downarrow +\varepsilon L\downarrow \tag{7}$$

where α is albedo, $S\downarrow$ is solar radiation (W/m^2) and $L\downarrow$ is downward long-wave radiation (W/m^2). The method of calculating each term in Equation 7 is explained here. Using the same methods as Nakayama *et al.* (10) and Lu *et al.* (11), solar radiation ($S\downarrow$) was calculated, using corrected slopes in the longitudinal and latitudinal directions. To estimate the solar radiation from the sunshine duration measured at the dam management site, this following equation was applied:

$$\frac{S\downarrow}{S_0\downarrow} = b_0 + b_1\left(\frac{N}{N_0}\right) \tag{8}$$

where $S_0\downarrow$ is solar radiation at the horizontal surface (W/m^2), N is sunshine duration (hr), and N_0 is maximum sunshine duration (hr). The coefficients b_0 and b_1 are 0.193 and 0.516, respectively. These values were obtained at the observation sites. For the slope, $S_0'\downarrow$, solar radiation at the slope surface, is used instead of S_0:

$$S_0'\downarrow = I_{00}\left(\frac{d_0}{d}\right)^2 \cos\theta' \tag{9}$$

where I_{00} is the insolation at the top of the atmosphere (W/m^2), d and d_0 are distance between the sun and the earth (m) and the average of that distance (m), respectively, and θ' is zenith angle with surface correction (rad), which is given by the following equation:

$$\begin{aligned}
&\cos\theta' = K_1\cos h + K_2\sin h + K_3\\
&K_1 = \cos\phi\cos\delta\cos\theta_1\cos\theta_2 + \sin\phi\cos\delta\sin\theta_1\cos\theta_2\\
&K_2 = \cos\delta\sin\theta_2\\
&K_3 = -\cos\phi\sin\delta\sin\theta_1\cos\theta_2 + \sin\phi\sin\delta\cos\theta_1\cos\theta_2
\end{aligned} \tag{10}$$

where h is the hour angle assuming that culmination hour is zero (rad), δ is declination of the sun (rad), ϕ is latitude (rad), θ_1 is ground slope angle in the north -south direction (in rad, with south-facing taking positive values), θ_2 is ground slope angle in the east -west direction (in rad, with west-facing taking positive values). Equation 10 was integrated between $-H_1$ (sunrise hour angle) and H_2 (sunset hour angle), and the result was divided by 2π to obtain the daily average of the cosine of the zenith angle:

$$\begin{aligned}
&\overline{\cos\theta}' = \frac{1}{2\pi}[K_1(\sin H_1 + \sin H_2) - K_2(\cos H_2 - \cos H_1) + K_3(H_2 + H_1)]\\
&H_1 = \cos^{-1}\left[\frac{-K_1K_3 + K_2\sqrt{K_1^2 + K_2^2 - K_3^2}}{K_1^2 + K_2^2}\right]\\
&H_2 = \cos^{-1}\left[\frac{-K_1K_3 - K_2\sqrt{K_1^2 + K_2^2 - K_3^2}}{K_1^2 + K_2^2}\right]
\end{aligned} \tag{11}$$

Equation 11 was substituted into Equation 9, and the calculated result was substituted into Equation 8 to obtain the daily average solar radiation on the slope.

Albedo was parameterized in relation to air temperature (Kuchizawa *et al.* (9)). Fig. 4 shows measurements of albedo and their estimated values at an observatory in the Jozankei Dam basin (a driftwood treatment plant), α that have been parameterized with respect to air temperature, T_a (°C) as shown in Equation 12.

$$\alpha = -0.020T_a + 0.554 \quad \text{at} \quad 0.40 < \alpha < 0.90 \tag{12}$$

Thus, the value of albedo varies greatly according to the presence or absence of snow, but Fig. 4 illustrates the fairly estimations of albedo values.

The downward long-wave radiation, $L\downarrow$, can be computed by the following equation:

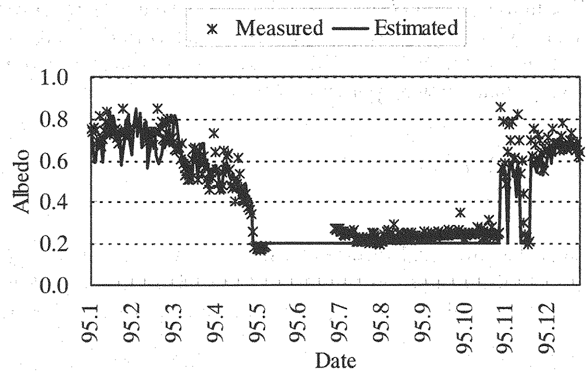

Fig. 4. Estimation of albedo (at the driftwood treatment plant from Jan. 1 to Dec. 31, 1995)

$$L\downarrow = \sigma T^4\left[1-\left(1-\frac{L_f\downarrow}{\sigma T^4}\right)C\right] \tag{13}$$

where $L_f\downarrow$ is downward long-wave radiation under clear sky (W/m^2), and C is a coefficient for the effects of clouds, T is air temperature (K) :

$$L_f\downarrow = (0.74+0.19x+0.07x^2)\sigma T^4, \qquad x=\log_{10}(0.14e) \tag{14}$$

$$C=\begin{cases}0.826A^3-1.234A^2+1.135A+0.298, & (0<A\le 1)\\ 0.02235, & (A=0)\end{cases} \tag{15}$$

where e is water vapor pressure (hPa), and A is the ratio of sunshine duration to maximum one(= N/N_0).

Q_G and Q_R in Equation 4 are expressed by Equations 16 and 17, respectively:

$$Q_G = Q_M + Q_S + Q_B \tag{16}$$

$$Q_R = 1.162RT_{wet} \tag{17}$$

where Q_M is heat flux expended to melt snow (W/m^2), Q_S is heat flux expended for snow temperature increase (=0), Q_B is heat flux supplied to the ground (W/m^2). The snowmelt amount on the ground surface was assumed to be 1 mm/d during the snow cover period (Arai (1), Kondo *et al.* (8)), -3.86 W/m^2 was assigned to Q_B. R is rainfall intensity (mm/h). T_{wet} is wet-bulb temperature (℃), but the air temperature during rainfall was assigned to this parameter for convenience.

Then, the mean temperatures of the two layers (T_g and T_v) were calculated from Equations 4 and 5, and sensible and latent heat fluxes were calculated by means of the bulk Equations 18 and 19.

$$H_g = C_p\rho C_{Hg}U\{T_g - T\}, \qquad H_v = C_p\rho C_{Hv}U\{T_v - T\} \tag{18}$$

$$lE_g = l\rho\beta_g C_{Hg}U\{e_{sat}(T_g)-e\}\frac{0.622}{P_0}, \quad lE_v = l\rho\beta_v C_{Hv}U\{e_{sat}(T_v)-e\}\frac{0.622}{P_0} \tag{19}$$

where C_p is specific heat at constant pressure (1,004 J/K/kg), ρ is density of air (kg/m^3), U is wind speed (m/s) at the specific elevation above ground, T is air temperature (K) at the specific elevation above ground, C_{Hg} and C_{Hv} are bulk coefficient at the ground surface and in the vegetation layer respectively, β_g and β_v are evaporation effectiveness factor at the ground surface and in the vegetation layer respectively, e_{sat} is saturate water vapor pressure (hPa), e is water vapor pressure (hPa) at the specific elevation above ground, and P_0 is pressure on ground (hPa).

Latent heat from interception evaporation, which is caused by precipitation, was estimated by means of the method using LAI (Kondo *et al.* (8)). Then, monthly values of LAI estimated by Ishii *et al.* (6)) were used.

Based on existing findings (Kondo *et al.* (8)), the values of bulk transport coefficient and evaporation efficiency of the ground surface, snow cover surface, vegetation layer, and other elements were set for consistency with the water balance method.

The long-term (several-year) average values of evapotranspiration were calculated by bulk equation (Equation 19) and equation for evaporation due to interception proposed by Kondo *et al.* (8). Thus, transpiration, E_v, evaporation due to interception, I and evaporation on ground surface, E_g are respectively shown in Table 1. The estimated values indicate that interception evaporation is a dominant factor, accounting for over 50% of all evapotranspiration. The evapotranspiration estimated in this study was roughly equal to the potential evapotranspiration obtained from the Thornthwaite and Penman equations under the same conditions.

Estimation of Snow Cover and Snowmelt

Whereas snowfall is added to snow cover amount, the amount of snowmelt and ground surface evapotranspiration are subtracted from it. To calculate the amount of snowmelt, the two-layer model is applied, and the calculation procedure is as follows:

1) T_g, obtained from Equations 4 and 5, is set equal to T_s, the tentative value for surface temperature of snow cover.
2) When T_s is 0 °C or below, snowmelt is assumed not to occur on the surface of snow cover. T_s, the tentative value for temperature of snow cover, is set equal to T_g. Following other findings (Kondo *et al.* (8), Arai (1)), the snowmelt amount from the bottom is assigned value of 1 mm/d.
3) When T_s exceeds 0 °C, then T_g and T_s are also set equal to 0 °C. The vegetation temperature under these conditions is given by Equation 5.
4) Q_M, the heat flux expended to snowmelt is calculated by Equations 4 and 16, and snowmelt amount is computed from that calculated value. In this case, the snowmelt amount from the bottom surface, Q_B is assigned the value of 1 mm/d, equivalent to energy of fusion of -3.86 W/m^2.

Next, factors related to snow cover are calculated. Based on the water balance of snow pack, the water equivalent of snow pack at a point in time (t) is formulated as follows:

$$S_w(t) = S_w(t-1) - \left(M(t) + E(t)\right) + \frac{\rho_{sf}}{\rho_w} S_f(t) \tag{20}$$

Depth and density of snow pack are given by following equations:

$$\begin{gathered} S_d(t) = \left[S_d(t-1) - \left(M(t) + E(t)\right) \frac{\rho_w}{\rho_s(t-1)} + S_f(t) \frac{\rho_{sf}}{\rho_s(t-1)} \right] \eta_s \\ \rho_s(t) = \frac{S_w(t)}{S_d(t)} \rho_w \end{gathered} \tag{21}$$

where S_w is water equivalent of snow pack (mm), S_d is depth of snow pack (mm), S_f is depth of snowfall (mm), M is snowmelt amount (mm), E is evapotranspiration (mm), ρ_w is water density (1,000 kg/m^3), ρ_s is density of snow pack (kg/m^3), ρ_{sf} is density of snowfall (160 kg/m^3), and η_s is mean compaction rate of the snow pack.

Yamazaki *et al.* (14) proposed a detailed model for compaction of snow pack, but our research employed a mean compaction rate for the snow pack layer, for the sake of simplicity. We assumed that this compaction rate is related to density of snow pack. Kinoshita (7) notes that the compaction rate increases with liquid water content, the liquid water acting as lubricous material. Thus, compaction rate were incorporated with respect to the density of snow pack by the values assumed to be 0.999 (for the lowest density of snow pack (309 kg/m^3)) and 0.985 (for the greatest density of snow pack (700 kg/m^3)).

As a result, the presence or absence of snow cover can be determined. The heat flux and evapotranspiration can be calculated based on this judgement, which is shown in Table 1. The ground surface conditions determine heat flux, as well as determining evapotranspiration and snowmelt. The results also show that the evaporation due to interception occupies more than the half of the total evapotranspiration. At an observatory in the Jozankei Dam basin (a driftwood treatment plant), changes in depth and density of snow were examined (Fig. 5). Fig. 6 shows estimated depths and densities at the dam management office of the two dam basins. Also, the snow depths measured by snow gauge and the snow densities measured by snow

Table 1. Evapotranspiration estimated by two-layer model (mean values from 1996 to 2000)

Basin	Transpiration	Evaporation due to interception	Evaporation on ground surface	Result from Two-layer model
Jozankei Dam	152	278	81	511
Hoheikyo Dam	181	282	110	573

Unit; mm/year

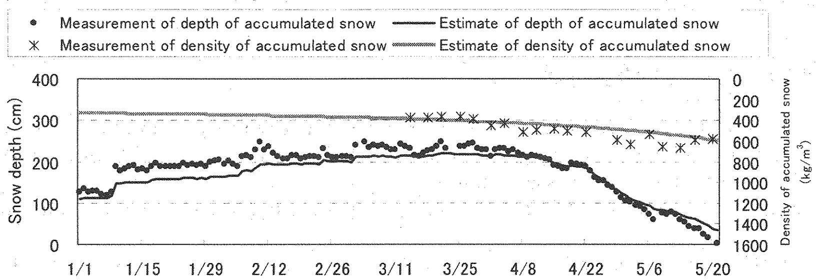

Fig. 5. Estimation of depth and density of snow
(at the driftwood treatment plant from Jan. 1 to May 21, 1996)

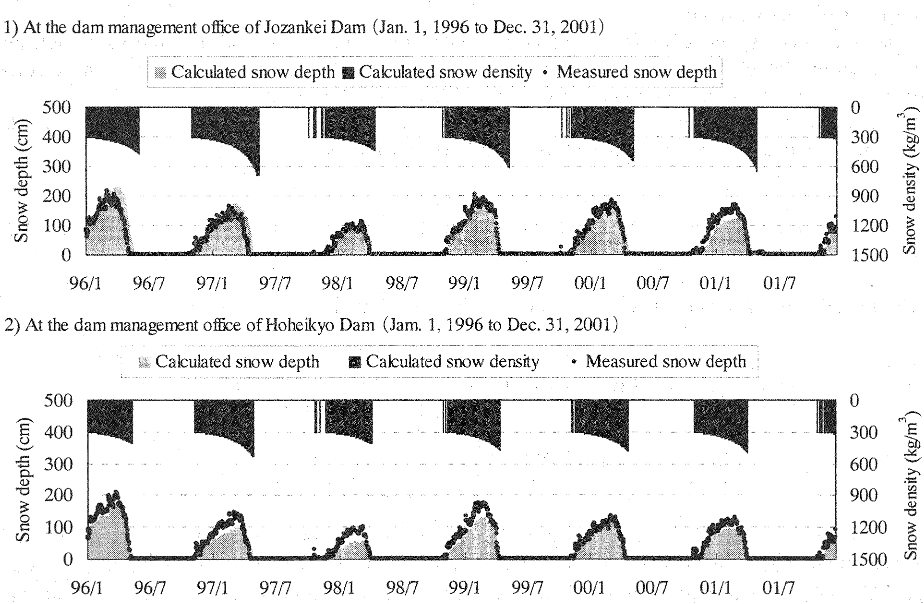

Fig. 6. Estimates of depth and density of snow pack

sampler with cross section of 8.24 cm^2 are shown. The point in time when the last snow melts are properly estimated for these two sites and the telemetry observation sites.

Fig. 7 compares the area of snow cover calculated by the model as of May 2, 2001 with that on the satellite image (LANDSAT-TM) on the same day. The snow cover area in the LANDSAT image was extracted under the conditions of BAND3-BAND4>0 and BAND4-BAND5>0 (where BAND3 is 0.63-0.69μm, BAND4 is 0.76-0.90μm, and BAND5 is 1.55-1.75μm). Figs. 5 and 6 show that the snow cover area is recreated fairly well by the water and heat balance model. The model properly quantifies not only snow depth for arbitrary selected locations, but also snow cover for the whole basin.

Assessment of Water Balance in the Basin

1) Jozankei Dam Basin 2/5/2001 2) Hoheikyo Dam Basin 2/5/2001

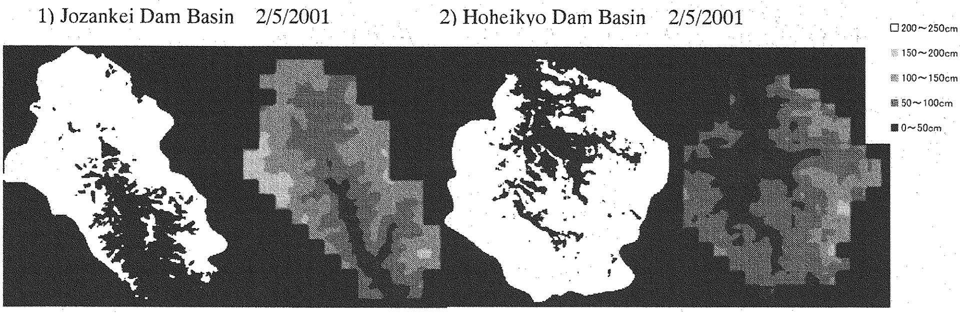

Fig. 7. Snow Cover Area by Satellite Image (left) and Calculation (right)

Table 2. Factors related to water balance of the two basins (mean values from 1996 to 2000)

Basin	Rainfall	Snowfall	Runoff	Evapotranspiration
Jozankei Dam	**811**	**1263**	**1569**	**505**
Hoheikyo Dam	**1043**	**1077**	**1604**	**516**

Unit; mm/year

Table 2 shows evapotranspiration, based on water balance, estimated from runoff and precipitation of the basin calculated in the previous paragraph as following equation.

$$E = R + M - Q - \Delta S \tag{22}$$

where E is evapotranspiration, R is rainfall (mm/yr), M is snowmelt (mm/yr), Q is runoff (mm/yr) and ΔS is change of storage amount in a watershed (mm/yr). In this case, ΔS can be canceled because the hydrological factors are averaged over a period of five years. The rainfall and snowfall of the Jozankei Dam basin differ from those of the Hoheikyo Dam basin. However, their evapotranspiration values are roughly equal, both slightly above 500 mm, as in the case of estimation by two-layer model (Table 1). The ratio of evapotranspiration to runoff is approximately 1 to 3, which agrees with the results from the other surveys on the Jozankei district (Hattori, (4)).

We note that characteristics of climate conditions are likely to relate to the percentage of precipitation that falls as snow. This percentage is about 60% in the Jozankei Dam basin, which is closer to the Sea of Japan than is the Hoheikyo Dam basin. It is approximately 50% at Hoheikyo Dam basin, which is closer to the Pacific Ocean than is the Jozankei Dam basin.

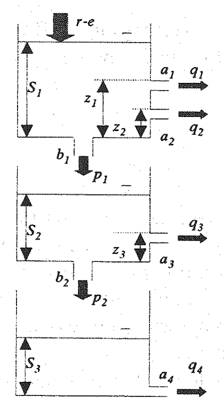

Fig. 8. Three-cascade Tank Model

RUNOFF ESTIMATION

Tank Model Parameter Identification Method

Fig. 8 schematically shows a three-cascade Tank Model for runoff estimation. This runoff model estimates runoff by recreating storage effects accurately. To determine parameters, a mathematical optimization method based on the Newton-Raphson method (Watanabe *et al.*, (13)) was employed.

It seems difficult to determine many parameters at one time. Therefore, we attempted a new approach to determine effectively the parameters. According to the method of Hino *et al.* (5) runoff can be separated into multiple components to produce an AR equation for each: groundwater runoff (q_G), subsurface runoff (q_M), and surface runoff (q_S). Runoff components can be separated by using the time constant obtained by an analysis of a regression part in the hydrograph. The groundwater runoff can be expressed by the following p^{th}-order AR equation:

$$q_G(k)=\sum_{i=1}^{p}A_{Gi}\cdot q_G(k-i)+B_G\cdot r_G(k-1),\qquad B_G=1-\sum_{i=1}^{p}A_{Gi} \tag{23}$$

where A_G is AR coefficient, and r_G is precipitation contributing to groundwater runoff.

Next, the Tank Model is formulated as follows:

$$\begin{aligned}&\frac{dS_1}{dt}=r_e-q_1-q_2-p_1,\ \frac{dS_2}{dt}=p_1-q_3-p_2,\ \frac{dS_3}{dt}=p_2-q_4,\\ &q_1=a_1(S_1-z_1),\ q_2=a_2(S_1-z_2),\ q_3=a_3(S_2-z_3),\ q_4=a_4S_3,\\ &p_1=b_1S_1,\ p_2=b_2S_2\end{aligned} \tag{24}$$

where q_1 to q_4 are runoff (mm/d), p_1 and p_2 are infiltration (mm/d), r_e is effective precipitation (= rainfall + snowmelt amount - evapotranspiration) (mm/d), and a_1, a_2, a_3, a_4, b_1, b_2, z_1, z_2 and z_3 are nine unknown parameters.

The storage amounts of the three cascade tanks can be obtained from solutions of first-order linear differential equations composed of these unknown parameters. The runoff of the three cascade tanks can be obtained as well. Substituting the value of S_3 into the first-order differential equation yields the following equation of groundwater runoff (q_4):

$$\frac{dq_4}{dt}=-a_4q_4+a_4p_2 \tag{25}$$

By solving the first-order linear differential equation for q_4, q_4 can be given in the form of a recurrence formula:

$$q_4(k)=\exp[-a_4t]\cdot q_4(k-1)+\{1-\exp[-a_4t]\}\cdot p_2(k-1) \tag{26}$$

Setting the coefficients of the input terms of Equation 23 (r_G) and Equation 26 (p_2) equal to each other yields the following equation:

$$a_4=-\frac{1}{t}\ln\left[\sum_{i=1}^{p}A_{Gi}\right] \tag{27}$$

where t is calculation time step (1 day). The process above shows that the parameter of groundwater runoff (a_4) can be determined by the AR coefficient. Supplementary use of the filter-separation AR method to determine parameters provides the following advantages: 1) a parameter can be determined for each separated component, and 2) some parameters can be determined first, for subsequent use to determine other unknown parameters. For example, when a parameter does not converge to any specific value, runoff can be separated into multiple components to determine parameters of each component. In our case, a_4 was determined first, which enabled us to determine eight other parameters at the same time.

In the Newton-Raphson method, which was employed to determine parameters, $\delta\mathbf{P}$, used for parameter convergence, needs to be given such that the objective function $J(\mathbf{P})$ takes its smallest value. The equation of $\delta\mathbf{P}$ is as follows:

$$J(\mathbf{P})=\frac{1}{N}\mathbf{e}^T(\mathbf{P})\mathbf{e}(\mathbf{P})=\frac{1}{N}\sum_j e_j^{\,2},\qquad e_j=\frac{\left|q_j^{\,*}-q_j(\mathbf{P})\right|}{\sqrt{q_j^{\,*}}} \tag{28}$$

$$\frac{\partial J(\mathbf{P}+\delta\mathbf{P})}{\partial(\delta\mathbf{P})}=0\Rightarrow\delta\mathbf{P}=-\left[\left(\frac{\partial\mathbf{e}}{\partial\mathbf{P}}\right)^T\left(\frac{\partial\mathbf{e}}{\partial\mathbf{P}}\right)\right]^{-1}\left[\left(\frac{\partial\mathbf{e}}{\partial\mathbf{P}}\right)^T\mathbf{e}(\mathbf{P})\right] \tag{29}$$

Table 3. Parameters related to the groundwater runoff (Aug. 1 to Oct. 31, 1998; a_4 was fixed)

	Factors of the groundwater runoff component			
	Time Constant (day)	**Order of AR equation**	**Total of AR coefficients**	a_4
Jozankei Dam	**70**	**4**	**0.915**	**0.089**
Hoheikyo Dam	**45**	**4**	**0.930**	**0.073**

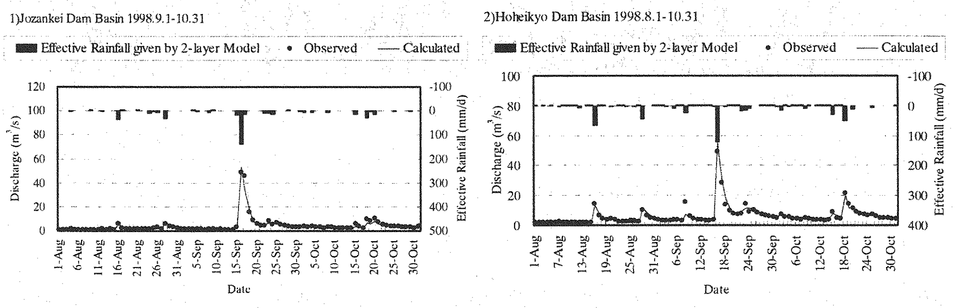

Fig. 9. Results of runoff analysis (August 1 to October 31, 1998)

Table 4. Identification process of parameters for Hoheikyo Dam basin (Aug.1 to Oct. 31, 1998; a_4 was fixed)

NO	a_1	a_2	a_3	a_4	b_1	b_2	z_1	z_2	z_3
1	0.5000	0.1000	0.1000	0.0730	0.1000	0.1000	30.0000	20.0000	20.0000
2	0.2113	0.1563	0.1000	0.0730	0.1283	0.1029	32.2500	17.1200	22.7100
3	0.2021	0.1587	0.1000	0.0730	0.1155	0.0969	41.5800	20.6100	23.5400
4	0.2605	0.1601	0.0109	0.0730	0.1080	0.1076	50.8700	21.6200	22.7200
5	0.3208	0.1427	0.0393	0.0730	0.1133	0.1036	51.5200	19.8300	45.5100
6	0.3178	0.1456	0.0393	0.0730	0.1020	0.0980	54.0000	20.9800	45.5100
7	0.3156	0.1458	0.0402	0.0730	0.1033	0.0978	53.7700	20.6900	45.6300
8	0.3157	0.1458	0.0407	0.0730	0.1035	0.0977	53.7400	20.6400	45.5700
9	0.3158	0.1458	0.0409	0.0730	0.1035	0.0976	53.7300	20.6300	45.5300
10	0.3158	0.1458	0.0410	0.0730	0.1035	0.0976	53.7200	20.6200	45.5300
11	0.3158	0.1458	0.0410	0.0730	0.1035	0.0976	53.7200	20.6200	45.5500
12	0.3158	0.1458	0.0410	0.0730	0.1036	0.0975	53.7200	20.6200	45.5500

where **P** is a 9x1-parameter vector, **e** is an Nx1-error vector (error of the j^{th} daily runoff data is e_j in Equation 28), N is the number of data, q is calculated runoff, and q^* is observed runoff. Since the derivative of the parameter of the error (Nx9 Jacobian matrix, $\partial \mathbf{e}/\partial \mathbf{P}$) can be analytically obtained, it is relatively easy to converge to optimum values.

Results of the Runoff Analysis

Data adopted for parameter determination for the two basins were the data on days with rainfall for the approximately three months (92 days) from August through October 1998. The parameters acquired are applied to calculation of long-term (several-year) runoff. Table 3 shows values of the parameters of the two dam basins and Fig. 9 shows runoff analysis results. The parameters for Hoheikyo Dam converge at the twelfth updating. Table 4 contains data related to groundwater runoff parameters. a_4, a constant in Table 3, has been calculated by the summation of AR coefficients using Equation 27. The root mean-square error (RMSE) of daily average runoff $((\Sigma(q_{cal}-q_{obs})^2/N)^{0.5})$ was 1.6 for the Jozankei Dam basin and 1.5 for the Hoheikyo Dam basin.

Results of long-term runoff calculation

The daily average runoff and storage amount are estimated by providing effective snowmelt and effective rainfall that does not include evapotranspiration (Fig. 10). The parameters were determined for only three

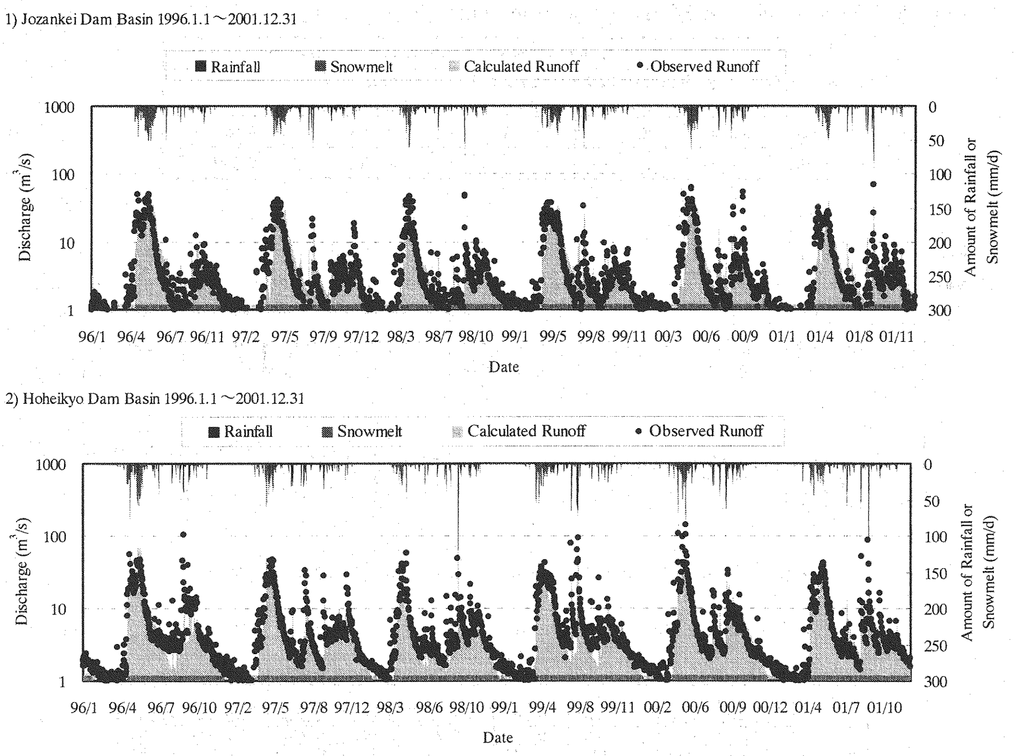

Fig. 10. Results of runoff calculation

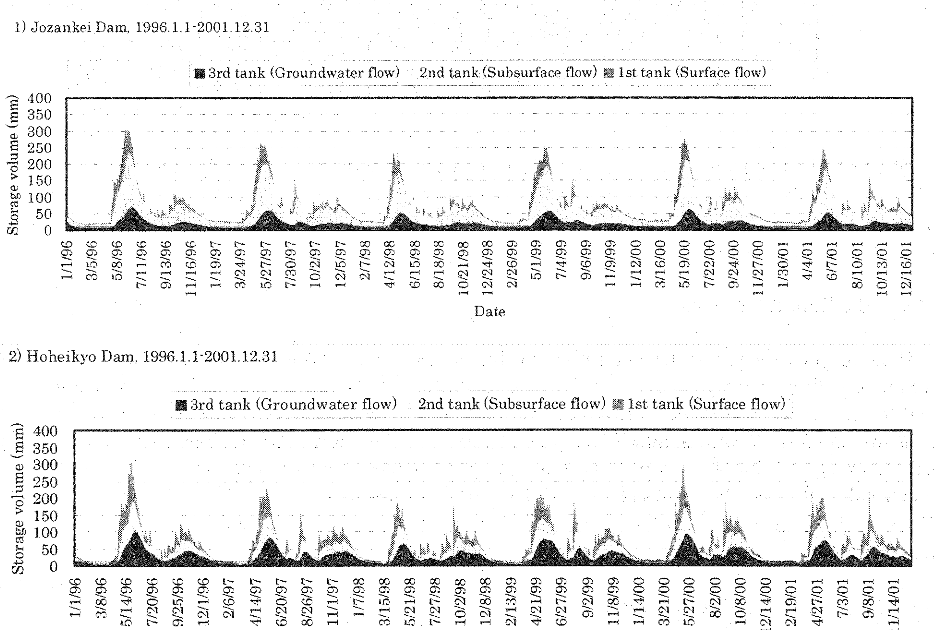

Fig. 11. Changes in storage amount of each component

months, but runoff for a long period, including the snowmelt period, is shown to be accurately estimated. When runoff suddenly increases, such as during periods of heavy rainfall, the model cannot adjust very well. In such situations, to deal with runoff, which is strongly affected by non-linear factors, temporal resolution must be calculated in detail.

Even the initial conditions for short-term flood runoff calculation should reflect the trends of storage amount and snow accumulation on the basis of proposed long-term runoff calculation. This will help to increase the calculation accuracy. Fig. 11 shows storage amounts of the two dam basins. The figure illustrates that groundwater storage amounts influence runoff in the Hoheikyo Dam basin. Thus, in addition to hydrological factors, the storage effect needs to be analyzed according to soil characteristics, such as quality and type.

SUMMARY

The summary is as follows:

1) A two-layer model was applied to comprehensive estimation of a series of hydrological factors (rainfall, factors related to snow cover, snowmelt, evapotranspiration) under the integrated conditions of water and heat fluxes. Change of snow cover and its effects were estimated in relation to the evaluation of hydrologic cycle.
2) Water and heat fluxes could be estimated for each basin by incorporating the effects of vegetation based on routine meteorological data.
3) Application of the Newton-Raphson method was found to be effective in determining the parameters for the Tank model. It was proven that parameters for groundwater runoff can be determined by a different method, in this case, by formulation using AR coefficient.
4) Because the Two-layer Model integrates the effects of changes in snow cover and the Tank Model was properly fine-tuned, the long-term hydrological factors and hydrologic cycle of a cold, snowy region were properly reproduced.

If the proposed method can be expanded to integrate the storage effects of snow cover and the ground, practical applications to water resource management and improvement of flood prediction accuracy can be anticipated.

ACKNOWLEDGEMENTS

This study was commissioned by the Hokkaido Development Bureau of the Ministry of Land, Infrastructure and Transport to whom we wish to express our gratitude.

REFERENCES

1. Arai, T.: Snowmelt and flood due to snowmelt, Chapter 3, Snow and ice hydrology, N. Maeno, and M. Fukuda, ed., Kokon Shoin Co., Ltd., Tokyo, Japan, pp.49-91, 1994 (in Japanese).
2. Bathurst, J.C., and K.R. Cooley : Use of the SHE hydrological modeling system to investigate basin response to snowmelt at Reynolds Creek, Idaho, J. Hydrology, Vol.175, pp.181-211, 1996.
3. Bras, R.L. : Hydrology, An introduction to hydrologic science, Addison-Wesley Publishing Company, INC., USA, pp.248-249, 1990.
4. Hattori, S. : Characteristics of hydrologic cycle in forest basin and forest management, Proc. 4th Seminar of Hydrology and Water Resources, pp.19-29, 2002 (in Japanese).
5. Hino, M., and M. Hasebe : Identification and prediction of nonlinear hydrologic systems by the filter-separation autoregressive (AR) method, Extension to hourly hydrologic data, J. Hydrology, Vol.68, pp.181-210, 1984.
6. Ishii, T., M. Nashimoto, and H. Shimogaki : Estimation of leaf area index using remote sensing data, J. Japan Soc. Hydrology & Water Resour., Vol.12, No.3, pp.210-220, 1999 (in Japanese with English summary).
7. Kinoshita, S : Compression of snow immersed in water of 0℃, I. Low Temperature Science, Ser. A, 21, pp.13-22, 1963 (in Japanese with English summary).
8. Kondo, J. ed. : Meteorology for water environment, Asakura Shuppan Co., Ltd., Tokyo, Japan, 1994 (in Japanese).
9. Kuchizawa, H., and M. Nakatsugawa : Estimation of snow pack condition and evapotranspiration based on water and heat balances in watershed, Monthly Report of Civil Engineering Research Institute, 588, pp.19-38, 2002 (in Japanese with English summary).

10. Nakayama, K., and S. Itoh, M. Fujita and D. Saitoh : Runoff analysis considering snowmelt in a mountainous River, J. Hydraulic, Coastal and Environmental Engineering, No.691, II-57, pp. 25-41, 2001.11 (in Japanese with English summary).
11. Lu, M., T. Koike and N. Hayakawa : Development of a distributed snowmelt analysis system using AMeDAS data and digital geographic information, Annual Journal of Hydraulic Engineering, JSCE, Vol.42, pp.121-126, 1998.2 (in Japanese with English summary).
12. Tanakamaru, H. : Parameter identification of Tank Model with the genetic algorithm, Annuals of the Disaster Prevention Research Institute, Kyoto University, No.36, B-2, pp.231-239, 1993 (in Japanese).
13. Watanabe, K., K. Tateya, K. Matsuki, and K. Hoshi : Refinements to parameter optimization in the Tank Model, Proc. of the 33rd Japanese Conference on Hydraulics, pp.55-60, 1989 (in Japanese with English summary).
14. Yamazaki, T., T. Sakuraoka, T. Nakamura, and J. Kondo : A study of snow metamorphism: I model description, Seppyo, 53, 2, pp.115-123, 1991 (in Japanese with English summary).

APPENDIX – NOTATION

The following symbols are used in this paper:

R = rainfall (mm/d);

S = snowfall depth (cm/d);

rh = relative humidity;

T_c = reference temperature for discriminating between snowfall and rainfall (℃);

f_v = transmissivity of the vegetation;

$R\downarrow$ = downward net radiation (W/m^2);

T_g, T_v = temperatures of ground surface and vegetation layer (K);

H_g, H_v = sensible heat fluxes from the ground surface and vegetation layer (W/m^2);

lE_g, lE_v = latent heat fluxes from the ground surface and vegetation layer (W/m^2);

lI = latent heat flux due to interception (m/s);

σ = Stefan-Boltzmann coefficient (5.67x10^8 W/m^2/K^4);

ε = emmissivity of the ground surface;

Q_G = heat flux provided to the ground surface (W/m^2);

Q_R = heat flux provided by rainfall (W/m^2);

LAI = leaf area index (m^2/m^2);

$S\downarrow$ = downward solar radiation (W/m^2);

$S_0'\downarrow$ = downward solar radiation at the slope surface under clear sky (W/m^2);

$L\downarrow$ = downward long-wave radiation (W/m^2);

α = albedo;

N = sunshine duration (hr);

I_{00} = insolation at the top of the atmosphere (W/m^2);

d = distance between the sun and the earth (m);

θ' = zenith angle with surface correction (rad);

H, δ, ϕ = hour angle, declination of the sun and latitude (rad);

θ_1, θ_2 = ground slope angles in the north-south and the east-west directions (rad);

H_1, H_2 = sunrise hour angle and sunset hour angle (rad);

T_a, T_{wet} = air temperature and wet-bulb temperature (℃);

$L_f\downarrow$ = downward long-wave radiation under clear sky (W/m^2);

C = coefficient for the effects of clouds (rad);

Q_M = heat flux expended to melt snow (W/m^2);

Q_S = heat flux expended for snow temperature increase (W/m^2);

Q_B = heat flux supplied to the ground (W/m^2);

e_{sat}, e = saturate water vapor pressure and water vapor pressure (hPa);

ρ = density of air (kg/m^3);

U = wind speed at the specific elevation above ground (m/s);

P_0 = pressure on ground (hPa);

T = air temperature at the specific elevation above ground (K);

C_{Hg}, C_{Hv} = bulk coefficients at the ground surface and in the vegetation layer;

β_g, β_v = evaporation effectiveness factors at the ground surface and in the vegetation layer;

E_g, E_v, = transpiration and evaporation on ground surface (m/s);

I = evaporation due to interception (m/s);

L = latent heat of vaporization (2.50x10^6 J/kg);

S_w, S_f, S_d = water equivalent of snow pack, depth of snow pack and depth of snowfall (mm);

M = snowmelt amount (mm);

E = evapotranspiration (mm);

ρ_w = water density (kg/m^3);

ρ_s, ρ_{sf} = density of snow pack and density of snowfall (kg/m^3);

η_s = compaction rate of snow pack ;

Q = runoff (mm);

ΔS = change of storage amount in a watershed (mm);

S = storage amount (mm);

r_e = effective precipitation (=rainfall + snowmelt – evapotranspiration) (mm/d);

q = runoff (mm/d);

p = infiltration (mm/d); and

a, b, z = parameters in the Tank model.

(Received May 14, 2004 ; revised July 23, 2004)